



HAL
open science

Stress-sensitivity of wafer-level packaged SAW delay lines

Lilia Arapan, Guillaume Wong, Bernard Dulmet, Thomas Baron, Jean-Michel Friedt, Vincent Placet, Sébastien Alzuaga

► **To cite this version:**

Lilia Arapan, Guillaume Wong, Bernard Dulmet, Thomas Baron, Jean-Michel Friedt, et al.. Stress-sensitivity of wafer-level packaged SAW delay lines. European Frequency and Time Forum, Apr 2016, York, United Kingdom. 10.1109/EFTF.2016.7477812 . hal-03427001

HAL Id: hal-03427001

<https://hal.science/hal-03427001>

Submitted on 12 Nov 2021

HAL is a multi-disciplinary open access archive for the deposit and dissemination of scientific research documents, whether they are published or not. The documents may come from teaching and research institutions in France or abroad, or from public or private research centers.

L'archive ouverte pluridisciplinaire **HAL**, est destinée au dépôt et à la diffusion de documents scientifiques de niveau recherche, publiés ou non, émanant des établissements d'enseignement et de recherche français ou étrangers, des laboratoires publics ou privés.

Stress-sensitivity of wafer-level packaged SAW delay lines

Lilia Arapan, Guillaume Wong, Bernard Dulmet, Thomas Baron, Jean-Michel Friedt, Vincent Placet, Sébastien Alzuaga

► **To cite this version:**

Lilia Arapan, Guillaume Wong, Bernard Dulmet, Thomas Baron, Jean-Michel Friedt, et al.. Stress-sensitivity of wafer-level packaged SAW delay lines. European Frequency and Time Forum, Apr 2016, York, United Kingdom. hal-03427001

HAL Id: hal-03427001

<https://hal.archives-ouvertes.fr/hal-03427001>

Submitted on 12 Nov 2021

HAL is a multi-disciplinary open access archive for the deposit and dissemination of scientific research documents, whether they are published or not. The documents may come from teaching and research institutions in France or abroad, or from public or private research centers.

L'archive ouverte pluridisciplinaire **HAL**, est destinée au dépôt et à la diffusion de documents scientifiques de niveau recherche, publiés ou non, émanant des établissements d'enseignement et de recherche français ou étrangers, des laboratoires publics ou privés.

Stress–Sensitivity of Wafer–Level Packaged SAW Delay Lines

Lilia Arapan, Guillaume Wong, Bernard Dulmet,
Thomas Baron, Jean-Michel Friedt, Vincent Placet
Time & Frequency Dpt,
FEMTO-ST, UMR CNRS-UFC-ENSMM-UTBM 6174,
26 Chemin de l’Épitaphe, 25030 Besançon, France
Email: lilia.arapan@femto-st.fr

Sébastien Alzuaga
SENSéOR, Besançon, France

Abstract—This paper presents the investigation of the influence of wafer-level packaging (WLP) on the stress–sensitivity of 100 and 200 MHz delay lines aimed to wireless sensing of stresses. The devices were fabricated on YXl/128° cut of lithium niobate. The investigated WLP achieves the assembly of two wafers by a 50 μm –thick layer of SU-8 photoresist. The delay line is micro-machined on top of the first wafer while the second wafer realizes the function of protective cap in a way that should not be detrimental to the stress-sensitivity of the device. The paper gives a comparison between the theoretical and experimental phase sensitivity of both packaged and raw devices submitted to a three–points bending test.

I. INTRODUCTION

Controlling the shift of parameters induced by the packaging is a key issue for the actual production of MEMS and SAW sensors initially developed in the laboratory. Here-studied devices are 100 MHz and 200 MHz delay lines on YXl/128° LiNbO₃. These devices are proof–of–concept samples close to higher–frequency sensors aimed to the wireless measurement of stresses in various kinds of structures. The actual wireless sensors are designed to operate in the 434 MHz and 2.45 GHz ISM bands. This circumstance puts significant constraints upon the microfabrication of the devices: wireless reading of SAW sensors is better achieved with high coupling piezoelectric substrate such as lithium niobate (LNO). The YXl/128° orientation, suitable for this purpose, fixes the Rayleigh wave velocity around 3990 m/s on a free surface, yielding a wavelength about 9 μm at 434 MHz and 1.6 μm at 2.45 GHz. Then the devices are fragile and must be encapsulated to protect them from external agents. Wafer Level Packaging (WLP) is a more efficient approach than Die Level Packaging (DLP), especially in view of stress sensing because standard ceramic enclosures used to encapsulate RF devices are essentially designed from electrical viewpoint, are not aimed to transmit the strain of the analyzed external structure to the SAW device, and induce strong thermally–induced differential stresses in the sensor. This issue is solved by the WLP technique consisting of assembling two wafers from the same material and dicing the chips at the very end of the fabrication process. The most common wafer-bonding techniques used in RF MEMS are direct surface bonding, glass frit and metallic layer bonding, achieving a rigid contact between the wafers. In case of bending, this features minimizes the extensional stresses at the interface, close to the neutral fiber of the assembly. Since

it coincides with the region of acoustic energy localization, such Wafer-Level Packaging (WLP) results into poor stress sensitivity of the sensors. Then, here–presented research was motivated by the need to reach a good compromise between the protection and the preservation of the stress sensitivity of the packaged delay lines.

II. DESIGN OF WAFER LEVEL PACKAGING

The most simple and generic WLP strategy relies on the assembly of 2 wafers of the same material and thickness. In such structure, traction-extension can be effectively transmitted along the entire cross-section of the assembly, but a flexural bending imposed by the monitored external structure has little chance to induce significant extensional strain and stress in the sensor if the surface acoustic wave propagates in the vicinity of the neutral fiber of the assembly. Conversely, by principle, the maximum longitudinal stress on the internal surface of a 2 wafers assembly is obtained when the sealing allows a perfect sliding between the wafers, as can be checked on Fig. 1 showing the FEA–computed distribution of the extensional strain ε_{xx} in the entire structure.

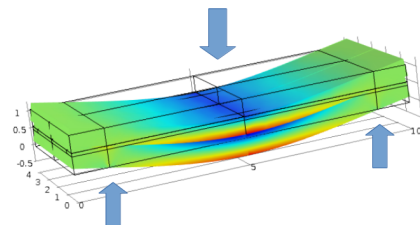


Fig. 1. Schematic distribution of extensional strain ε_{xx} for a three–points bending experiment applied to a typical two–wafers assembly with a sliding contact at the periphery. A 20 N net transverse force induces a value of ε_{xx} about $5.6 \cdot 10^{-4}$ at the upper surface of the base layer. Upon applying rigid contact conditions, the longitudinal strain drops to $1.8 \cdot 10^{-4}$.

We investigated the possibility to improve the stress–sensitivity of the packaged devices by realizing a soft polymer seal between the two wafers of the assembly. The moderate stiffness of the polymer joined with a sufficient thickness is expected to significantly soften the mechanical link between the two LNO layers, thereby increasing the longitudinal strain and stress at the free surface of the delay line wafer, in order

to improve the stress–sensitivity of the packaged device. In this purpose, a seal consisting of a $50\ \mu\text{m}$ –thick layer of SU–8 photoresist was found worth investigating, while eliminating the need of any additional etching operation to permit the free propagation of the SAW on top of the base wafer. The delay line systems consisted of one IDT transducer with 10 finger pairs plus two short reflectors on the measurement path and another one on the opposite side of the IDT for calibration of the time delay. The period of the IDT is $40\ \mu\text{m}$ for the test samples operating near 100 MHz, and $20\ \mu\text{m}$ for the samples operating near 200 MHz.

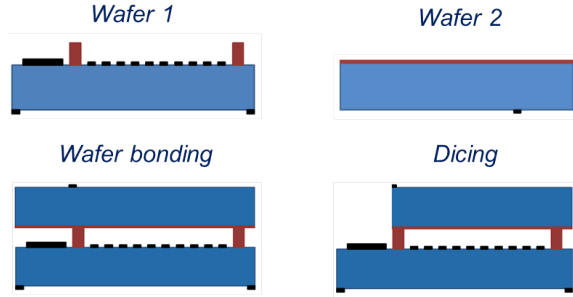


Fig. 2. Principle of soft polymer assembly for here–studied WLP design.

The fabrication process of the devices is illustrated on Fig. 2. Its main steps are the following:

a) Processing of Wafer 1 (device):

- Patterning the delay lines (Au deposit).
- Sputtering a thicker layer for the contact pads aimed to receive antennas after processing the WLP.
- Patterning of crosses to guide the dicing operation to separate the packaged die at the final step.
- Deposit and patterning of the $50\ \mu\text{m}$ –thick layer of SU–8 2075 polymer photoresist.

b) Processing of Wafer 2 (cap):

- Patterning dicing crosses (Au) to guide the dicing of the cap layer, aimed to provide access to the antennas contact pads.
- Spin-coat a thin layer of SU–8 2002 on the entire surface, in order to permit mutual adhesion by pressure and moderate heating.

c) Assembly and final operations:

- Wafers alignment and bonding.
- Dicing of wafer 2 to expose the contact pads.
- Dicing the entire thickness of the assembly in order to separate the chips.

III. PHASE-SHIFT MEASUREMENT UNDER 3-POINTS BENDING LOAD EXPERIMENT

Three–points bending tests were performed on both packaged and unpackaged chips with a traction machine of the



Fig. 3. Three–points bending experiment of a packaged chip (inside the ellipse mark).

Applied Mechanics Dpt. of FEMTO–ST. The electrical response was recorded during various transverse load cycles back and forth between 0 and $40\ \text{N}$. The packaged samples broke upon application of a transverse load threshold near $45\ \text{N}$. Fig. 4 shows typical response of a 200 MHz packaged device.

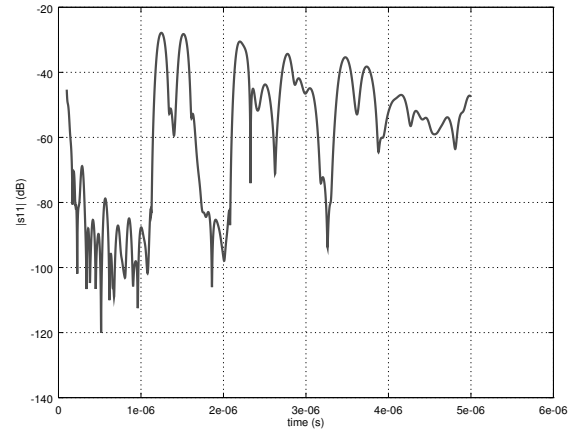


Fig. 4. $|s_{11}|$ electrical response of a 200 MHz packaged delay line.

The echoes correspond to the successive reflexions on the 3 reflectors present on the devices, including multiple reflexions along the acoustical path. The corresponding phase response is shown on Fig. 5. The phase behavior is altogether linear in the vicinity of the amplitude peaks. Then we selected the stress–induced phase change at $1.2\ \mu\text{s}$, $1.4\ \mu\text{s}$, $2.1\ \mu\text{s}$, and $2.7\ \mu\text{s}$ to plot the force–sensitivity characteristics shown on Fig. 6.

IV. ANALYSIS OF RESULTS

The relative phase shift is related to the bias–induced velocity shift and the time delay by the following chain of relationships:

$$\delta\varphi = \omega\delta\tau = \omega\delta\left(\frac{L}{V}\right) = -\frac{\omega L}{V^2}\delta V = -\omega\tau\frac{\delta V}{V} \quad (1)$$

where φ denotes the phase of the response at a fixed observation point, V denotes the phase velocity of the surface wave, τ is the time delay and L is the distance travelled by the wave. Since velocity is scalar and static strain and stress as well are

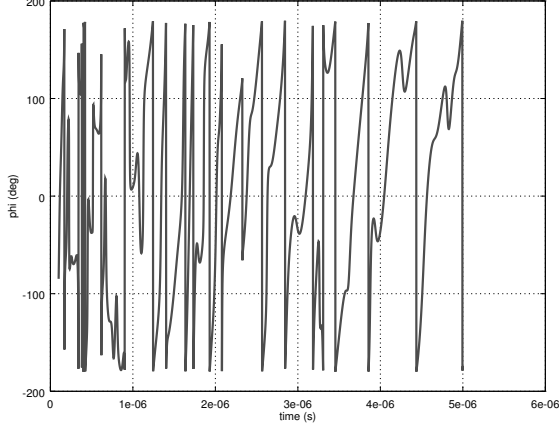


Fig. 5. Phase response of a 200 MHz packaged delay line.

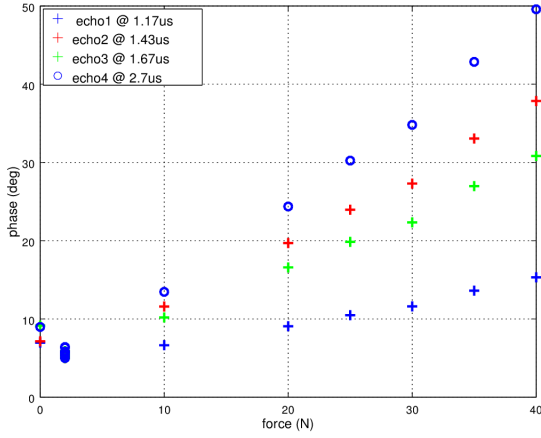


Fig. 6. Phase-shift v.s force characteristics of different echoes.

second rank tensors, the velocity shift is related to strain and stress by second rank pseudo-tensors¹, for instance:

$$\frac{\delta V}{V} = \alpha_{KL} \sigma_{KL} \text{ or } \frac{\delta V}{V} = \beta_{KL} \bar{E}_{KL} \quad (2)$$

where σ and \bar{E} respectively denote the static stress and strain, whereas α and β merely define the stress- and strain-sensitivity coefficients of the surface wave. These formulas hold only for uniform biases. The calculation of stress-sensitivity coefficients can be found in [1], [2] for the purely elastic problems but can also be derived for piezoelectric problems. Before proceeding further, we find enlightening and even necessary to consider the global context of the so-called acousto-elastic effect ruling the propagation of small-amplitudes elastic waves in a biased structure. Acousto-elastic effect and related problems were the subject of an

¹Although the value of the wave velocity is scalar, it is defined as the norm of the vector $\partial \bar{u} / \partial t$ where \bar{u} is the particular displacement. Then V depends on the orientation of the propagation on the semi-infinite substrate and this must be taken into account when calculating the stress-sensitivity coefficients. Thus α is not a tensor... unless we consider it is defined for the unique problem of the YX1-/128°SAW propagation in lithium niobate.

abundant literature in the second half of the 20-th century and constitute a particular application of the non linear theory of thermo-electro-elasticity in finite deformation. We illustrate below some of its aspects of interest for our purposes, while restricting here-presented formulas to the purely elastic case, for the sake of clarity and simplicity. Actually we performed all our numerical computations by taking into account the effect of the bias on the elastic part of the complete piezoelectric problem. In other words, we ignore bias-induced effects on the piezoelectric and dielectric behavior, although Rayleigh waves velocity is computed in the framework of piezoelectricity. Here we follow the well-established Lagrangian approach of small fields superimposed onto a bias [3], [4]. Then the propagation equations of surface waves [5] on a semi-infinite substrate of normal \bar{n}_2 in a current frame, rotated w.r.t crystallographic axes, can be mapped onto the set of fixed and known material coordinates (X_L) of the structure defined prior exertion of any bias:

$$\begin{aligned} \tilde{K}_{1\gamma,1} + \tilde{K}_{2\gamma,2} &= \rho_0 \ddot{u}_\gamma, \quad \gamma \in [1, 2, 3] \\ \tilde{K}_{L\gamma} &= G_{L\gamma 1\epsilon} u_{\epsilon,1} + G_{L\gamma 2\epsilon} u_{\epsilon,2} \\ G_{L\gamma M\epsilon} &= c_{L\gamma M\epsilon} + \hat{c}_{L\gamma M\epsilon}(w_{P,Q}) \\ \hat{c}_{L\gamma M\epsilon}(w_{P,Q}) &= \bar{T}_{LM} \delta_{\gamma\epsilon} + c_{L\gamma M\epsilon PQ}^3 \bar{E}_{PQ} \\ &\quad + c_{L\gamma MK}^2 w_{\epsilon,K} + c_{LKM\epsilon}^2 w_{\gamma,K} \\ \bar{T}_{LM} &= c_{LMNP} w_{N,P} = c_{LMNP} \bar{E}_{NP} \end{aligned} \quad (3)$$

where $\bar{u}(X_L, t)$ is the dynamic displacement field, $\bar{w}(X_L)$ is the static displacement field (bias) and ρ_0 is the mass density of the undeformed body since the problem is mapped onto the fixed material coordinates. Also $\tilde{K}_{L\gamma}$ denotes the first Piola-Kirchhoff stress tensor and $G_{L\gamma M\epsilon}$ indicates a component of the effective elastic coefficients in the so-called Lagrangian configuration. Then one should solve these equations together with the associated boundary conditions prescribed on the free surface of normal \bar{n}_2^0 that we consider located at $X_2 = 0$:

$$\tilde{K}_{2\gamma}(X_1, 0) = 0, \quad \gamma \in [1, 2, 3]. \quad (4)$$

Although Eq. (3) initially puts the bias-induced incremental elastic constant $\hat{c}_{LKM\epsilon}$ as a function of the static displacement gradients $w_{M,N}$ it is possible to reformulate \hat{c} as a function of the static strain

$$\begin{aligned} \hat{c}_{L\gamma M\epsilon} &= \bar{T}_{LM} \delta_{\gamma\epsilon} + c_{L\gamma M\epsilon AB}^3 \bar{E}_{AB} \\ &\quad + c_{L\gamma MN}^2 \bar{E}_{\epsilon N} + c_{LNM\epsilon}^2 \bar{E}_{\gamma N}. \end{aligned} \quad (5)$$

Because the static stress tensor is easily deduced from the static strain by inverting the tensor of second order elastic constants c^2 , it is easy to further rewrite the \hat{c} increment of elastic constants as a linear combination of the static stresses, which we find unnecessary to explicitly reproduce here. Because its linear expansion must be performed in terms of the displacement gradients which are non-symmetrical, instead of the classical strains which are symmetrical, the first Piola-Kirchhoff tensor $\tilde{K}_{L\gamma}$ is asymmetric by nature. Then it must be stored in a matrix of dimension $[9 \times 9]$. In case of stress-free bias such as free thermal expansion, it has been demonstrated that this matrix remains symmetric [6] provided that the notations be properly chosen. Nevertheless, the expression of the bias-induced increments $\hat{c}_{L\gamma M\epsilon}$ clearly

indicates that in case of a stress-generating or simply non-uniform bias, the resulting \mathbf{G} matrix is no more symmetrical. Then, two approaches can be followed to compute the velocity of the surface acoustic waves from the incremental equations of motion:

- For uniform biases and some cases of non-uniform but rather simple biases, it is still possible to directly solve the equations following the same procedure as in linear elasticity problems, as long as the $[9 \times 9]$ size of the $[\mathbf{G}]$ matrix and its eventual asymmetry induce relatively small changes in the classical procedure.
- A first order perturbation procedure [7] involving the computation of integrals relying on the knowledge of the partial derivatives of the unperturbed (unbiased) displacement field and of the static (biasing) displacement field.

The problem of SAW propagation in rectangular plates submitted to pure extensional or pure bending biases can be solved with either one approach. Ref. [5] provides with a detailed comparison of the direct and perturbation approaches to compute the velocity shift of Rayleigh waves in a purely bended structure. For here-presented work, we designed a computer program able to numerically determine the velocity of the SAW for the $YXl/128^\circ$ orientation of a LiNbO_3 plate submitted to a uniform bias, and in particular in the case of a pure longitudinal stress. Despite of the bias, the structure of the Rayleigh waves could still be assumed to comply with the classical combination obtained in case of propagation on a unbiased substrate:

$$u_i = \left(\sum_{n=1}^4 C_n \beta_i^{(n)} e^{j\omega s_2^{(n)} x_2} \right) e^{j\omega(s_1 x_1 - t)}, \quad (6)$$

where C_n represents the weight of a given partial wave in the combination, $\beta_i^{(n)}$ is a component of the normalized amplitude vector of the n -th partial wave, s_1 is the slowness of the guided propagation and $s_2(n)$ is the slowness of the partial wave in the vertical direction. We intend to provide more details about the direct approach in a further paper. The obtained value of the velocity-shift was found about 80% of the value provided by an earlier program elaborated at LPMO laboratory at the end of the nineties [1], [2]. The latter program is based on simplifications occurring in Tiersten's perturbation integral for the computation of Rayleigh velocity [8] in the case of uniform elastic bias. The perturbation formula for the two-dimensional problem of the proagation of Rayleigh waves of quasi-infinite aperture is the following:

$$\frac{\delta V}{V_0} \approx \frac{\int_{S_0} \hat{c}_{L\gamma M \varepsilon}(w_{M,N}) \mathcal{R}(u_{\varepsilon,M}^0 u_{\gamma,L}^{0*}) dS_0}{2\rho_0 \omega^2 \int_{S_0} \mathcal{R}(u_\alpha^0 u_\alpha^{0*}) dS_0}, \quad (7)$$

where \mathcal{R} denotes the real part, the superscript * denotes the complex conjugate, S_0 being the sagittal plane. In case of a uniform bias, the integrals can be reduced to simpler integrals

over the depth of the semi-infinite substrate:

$$\frac{\delta V}{V_0} = \frac{\hat{c}_{L\gamma M \varepsilon} \int_{-\infty}^0 u_{\varepsilon,M}^0 u_{\gamma,L}^{0*} dx_2}{2\rho_0 \omega^2 \int_{-\infty}^0 u_\alpha^0 u_\alpha^{0*} dx_2}. \quad (8)$$

Because of the exponential character and the convergence in the depth of the substrate of the partial waves (6) entering the structure of Rayleigh waves, the integrals are easily calculated, leading to the final result:

$$\frac{\delta V}{V_0} = \frac{\sum_{L=1}^2 \sum_{\gamma=1}^3 \sum_{M=1}^2 \sum_{\varepsilon=1}^3 \hat{c}_{L\gamma M \varepsilon} \sum_{n=1}^4 \sum_{m=1}^4 \frac{C_n C_m^* \beta_\varepsilon^{(n)} \beta_\gamma^{(m)*} s_M^{(n)} s_L^{(m)*}}{s_2^{(n)} - s_2^{(m)*}}}{2\rho_0 \sum_{\alpha=1}^3 \sum_{n=1}^4 \sum_{m=1}^4 \frac{C_n C_m^* \beta_\alpha^{(n)} \beta_\alpha^{(m)*}}{s_2^{(n)} - s_2^{(m)*}}} \quad (9)$$

The stress-sensitivity coefficients α_{LM} introduced at Eq. (2) are easily computed from both this expression and (5). Using the set of elastic constants provided by Ref. [9] gives the following value of σ_{xx} stress-sensitivity coefficient of Rayleigh wave velocity for the considered problem:

$$\alpha_{11} \approx -4.257 \cdot 10^{-11} / Pa \quad (10)$$

The FEA-computed stress for the 3 points bending test on top of the packaged delay line wafer was found close to $-3.2 \cdot 10^7 Pa$ when the net transverse force reached 20 N and assuming a rigid contact of the polymer with the 2 layers of niobate. Substituting this value together with (10) into (2) and the obtained result back into (1) yielded a phase-shift of 20° for the fourth echo ($\tau \approx 2.7 \mu s$) of the phase-response. The corresponding measurement of $\delta\varphi$ observed on Fig. 6 for this point was 23° . Then the agreement between theory and experiment was found good. Assuming that the polymer-niobate contact allows a free sliding, which corresponds to the "ideal" case of Fig. 1 yielded a FEA-computed value $\sigma_{xx} \approx 1.47 \cdot 10^8 Pa$ at the surface of the chip. Then the corresponding predicted sensitivity becomes nearly 5 times larger than the one that we actually observed. Nevertheless a further experiment was required, given the variability of results between direct and perturbation approach, the even larger variability induced by the values of elastic constants (nearly a factor 2 between the results calculated from [10] and [9]) and the expectable unaccuracy arising from the simplifying assumption of the essential contribution of the stresses near the surface. Then another three-points bending test was performed with a raw (unpackaged) chip. In that case the chip was flip-flopped in the traction apparatus in order to permit the free propagation of the SAW. The force had to be reduced since the chip broke at a much smaller transverse load (near 25 N), as expected. We performed the calculation for the same echo at $2.7 \mu s$ as previously and for a transverse force equal to 9 N , giving a FEA-computed longitudinal stress $\sigma_{xx} \approx 2.4 \cdot 10^8 Pa$. Then, using the same computation procedure as previously, we obtained a theoretical phase-shift close to -180° , whereas the measured value was found close to -195° . The similar agreement between theory and experiment for the cases of the packaged and the raw chips confirms to a large extent the validity of the approach and the conclusion drawn about the rather adhesive link between the polymer layer and the lithium niobate wafers.

V. CONCLUSION

Here-presented study indicated a satisfactory agreement between calculated and measured values of the phase-shift of the response of packaged and raw delay lines under a transverse load, assuming that the polymer used to perform the WLP assembly achieves a rigid link with the two wafers of lithium niobate. The loss of sensitivity between a firm contact and a sliding contact at the interfaces is about 5, and the sliding contact case would still represent a loss of a factor 2 with respect to the raw chip, which seems unavoidable if the two wafers have the same thickness, since two identical plates in parallel double the stiffness with respect to a single plate. Then a further optimization of the packaging is still needed to improve the stress-sensitivity of the device in case of bending imposed by the supporting structure. Nevertheless, this WLP design is promising since the stress-sensitivity is still largely measurable in case of pure bending of the chip. In addition, one must point out that the actual biasing states imposed to the SAW sensor by the monitored structures are combinations of bending and extension-compression rather than pure flexure.

ACKNOWLEDGMENT

The authors would like to thank the LAbEX ACTION for the postdoctoral support of L. Arapan through the ECCO project and the DGA for the support of the PhD of G. Wong through the ALCASAR/LANCASTER project.

REFERENCES

- [1] D. Hauden E. Bigler, G. Théobald. Stress-sensitivity mapping for surface acoustic waves on quartz. *IEEE Trans. on Ultrasonics, Ferroelectrics, and Frequency Control*, 36:57–62, 1989.
- [2] S. Ballandras E. Bigler. Stress sensitivity coefficients: a general approach for bulk, rayleigh and surface transverse waves. *Proc. of IEEE Int. Freq. Contr. Symp. (IFCS)*, pages 422–429, 1996.
- [3] H. F. Tiersten. On the nonlinear equations of thermo-electroelasticity. *Int. J. Engng Sci.*, 9:587–604, 1971.
- [4] J. C. Baumhauer and H. F. Tiersten. Non linear electroelastic equations for small fields superposed on a bias. *J. Acoust. Soc. Am.*, 54(4):1017–1034, 1973.
- [5] B.K. Sinha and H.F. Tiersten. On the influence of a flexural biasing state on the velocity of piezoelectric surface waves. *Wave Motion 1*, pages 37–51, 1979.
- [6] Bernard Dulmet and Roger Bourquin. Lagrangian effective material constants for the modeling of thermal behavior of acoustic waves in piezoelectric crystals. i. theory. *J. Acoust. Soc. Am.*, 110(4):1792–1799, 2001.
- [7] H. F. Tiersten. Perturbation theory for linear electroelastic equations for small fields superposed on a bias. *J. Acoust. Soc. Am.*, 64(3):832–837, 1978.
- [8] H. F. Tiersten and B. K. Sinha. A perturbation analysis of the attenuation and dispersion of surface waves. *J. Appl. Phys.*, 49(11):87–95, 1978.
- [9] M. Onoe A. Warner and G. Coquin. Determination of elastic and piezoelectric constants for crystals in class (3m). *J. Acoust. Soc. Am.*, 42:1223–1331, 1967.
- [10] Yasuo Cho and Kazuhiko Yamanouchi. Non linear, elastic, piezoelectric, electrostrictive, and dielectric constants of lithium niobate. *J. Appl. Phys.*, 61:875–887, 1987.